Science and Technology Indonesia
e-ISSN:2580-4391 *p*-ISSN:2580-4405
Vol. 8, No. 1, January 2023

Research Paper

Enhanced Effectiveness on Phenol Removal by MgCr-LDH/Microcrystalline Cellulose Composite and Regeneration Study with Green Desorption Reagent

Nova Yuliasari[1*], Alfan Wijaya[2], Risfidian Mohadi[2,3], Aldes Lesbani[2,3]

[1]*Doctoral Program, Faculty of Mathematics and Natural Sciences, Sriwijaya University, Palembang, 30139, Indonesia*
[2]*Research Centre of Inorganic Materials and Coordination Complexes, Faculty of Mathematics and Natural Sciences, Sriwijaya University, Palembang, 30139, Indonesia*
[3]*Graduate School of Mathematics and Natural Sciences, Sriwijaya University, Palembang 30139, Indonesia*
***Corresponding author**: nova_yuliasari@unsri.ac.id

Abstract
Modified MgCr-LDH with microcrystalline cellulose (MgCr/MCC) was successfully prepared by the coprecipitation method and characterized using XRD, FT-IR, and BET analyses. MgCr/MCC showed an increase in surface area from 21.51 to 26.056 m^2/g. The material was tested as an adsorbent for the removal of phenol. MgCr/MCC showed an increase in adsorption capacity from the initial material of 24.631 to 58.480 mg/g. The optimum pH was at pH 9 and the adsorption process's equilibrium time is 70 minutes. The correlation coefficients on the kinetics and isotherm parameters show that phenol removal follows the pseudo second order (PSO) and Langmuir models with spontaneous and endothermic adsorption processes. The regeneration ability of MgCr/MCC material using the water-assisted ultrasonic system as a green desorption reagent was 3 cycles with a percent regeneration efficiency of 39.45%.

Keywords
LDH, Microcrystalline Cellulose, Phenol, Adsorption, Desorption, Regeneration

Received: 10 October 2022, Accepted: 14 January 2023
https://doi.org/10.26554/sti.2023.8.1.151-159

1. INTRODUCTION

The development of chemical industry plants has produced a lot of wastewater production from by-products. Phenol is a widely used organic compound found in major industrial effluents including petroleum, kerosene, textile industry, dyeing, resin manufacturing, and pharmaceutical industries (Rajamohan et al., 2022; Mahmoud et al., 2022). If wastewater containing phenol compounds is released into the environment without prior treatment, it will be exposed to aquatic organisms and humans. Reports confirm that concentrations of 1-2 mg/L of phenol are toxic to aquatic organisms such as fish, and concentrations of 10-100 mg/L are toxic to most aquatic organisms. Phenol is also acutely toxic to humans. Phenol is a toxic organic pollutant that is difficult to degrade (Zhao et al., 2022; Wang et al., 2020). Based on that, it is necessary to have an effective method for processing in the removal of phenol compounds. In recent years, a variety of different methods have been investigated for phenol removal. The effective method in phenol removal is the adsorption method due to its cost-effectiveness, environmental friendliness, flexibility, simplicity, and high performance (Lammini et al., 2022; Haydari et al., 2023; Hasanah et al., 2022b).

Layered double hydroxide (LDH) is a new and widely used adsorption material in organic pollutant removal due to its rich diversity, controllable layer spacing, and high adsorption capacity (Li et al., 2020; Abrishamkar et al., 2022). However, LDH has a weakness in its structure when regenerating the adsorbent so that it can reduce its adsorption capacity. This can be overcome by modifying LDH material with carbon-based material to improve the material performance in terms of adsorption capacity and the material structure is more stable during the adsorbent regeneration process. Research conducted by Ahmad et al. (2023), modified MgAl-LDH with activated charcoal which resulted in a high increase in surface area from 8.963 to 1449.02 m^2/g and adsorption capacity of direct yellow removal from 101.010 to 133.333 mg/g. Research conducted by Hasanah et al. (2022a), modified NiAl-LDH material with hydrochar from *Nephelium Lappaceum* Peel, resulted in an increase in adsorption capacity in the removal of congo red dyes by 246.43 from 61.728 mg/g in the pristine material and resulted in the regeneration ability of adsorbents as much as 4 cycles. Research that has been carried out by Iftekhar et al. (2017) resulted in a large adsorption capacity in the adsorption of rare earth elements (Y^{3+}) of 102.25 mg/g and resulted in the ability to regenerate adsorbents as much as 5 cycles using

ZnAl-LDH modification material with cellulose.

In this research, MgCr-LDH material was modified with carbon-based material, namely microcrystalline cellulose (MCC). MCC has attractive advantages including its non-toxic properties, biocompatibility, physical characteristics, abundant availability, biodegradability, high mechanical strength, and low cost. MMC can be applied as a potential material in various applications including wastewater treatment. MCC-modified materials will improve material performance including adsorption capacity, mechanical strength, and structural stability (Mubarak et al., 2022; Cho et al., 2022). Wijaya et al. (2022) modified the ZnCr-LDH material with cellulose which resulted in an increase in surface area from 0.133 m^2/g to 3.714 m^2/g, and resulted in an increase in adsorption capacity of 13.263 mg/g to 30.96 mg/g, and resulted in the ability to regenerate the adsorbent for 4 cycles.

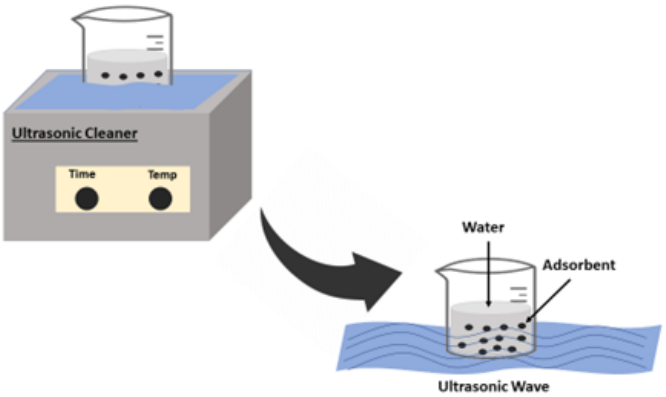

Figure 1. Schematic Desorption Process Using Water-assisted Ultrasonic Systems

One of the advantages of adsorbent materials that are widely reported is materials with high adsorption and regeneration capabilities. The regeneration process is carried out after the desorption process first. Many studies have been reported using desorption reagents in the form of chemical reagents that are not environmentally friendly such as ethanol, methanol, and sodium hydroxide (Da Silva et al., 2022; Qu et al., 2022; Said et al., 2021). The use of desorption reagents in the form of chemical reagents will indeed desorb the adsorbate maximally but will cause new problems, namely the remaining reagents after the desorption process which will make new waste. In this study, desorption process was carried out using an environmentally friendly reagent, namely water assisted by an ultrasonic system (Figure 1).

In this work, the preparation of MgCr/MCC composite materials was carried out by co-precipitation method and investigated by several characterization data, including XRD, FT-IR, and BET analyses. The material will be applied to the removal of phenol. The pH pzc, effect of pH, adsorption contact time, effects of initial concentration and temperature on the adsorption process, and regeneration study with green desorption reagent were some of the treatments and parameters used in this investigation.

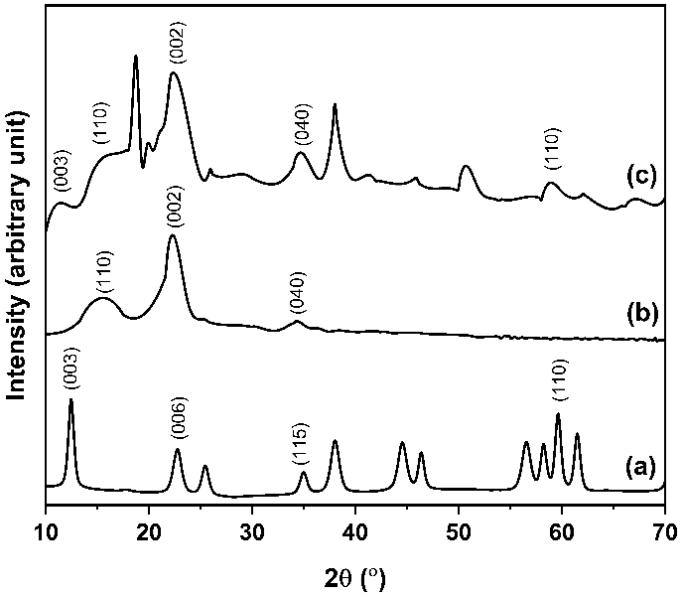

Figure 2. XRD Pattern of MgCr-LDH (a), MCC, and MgCr/MCC (c)

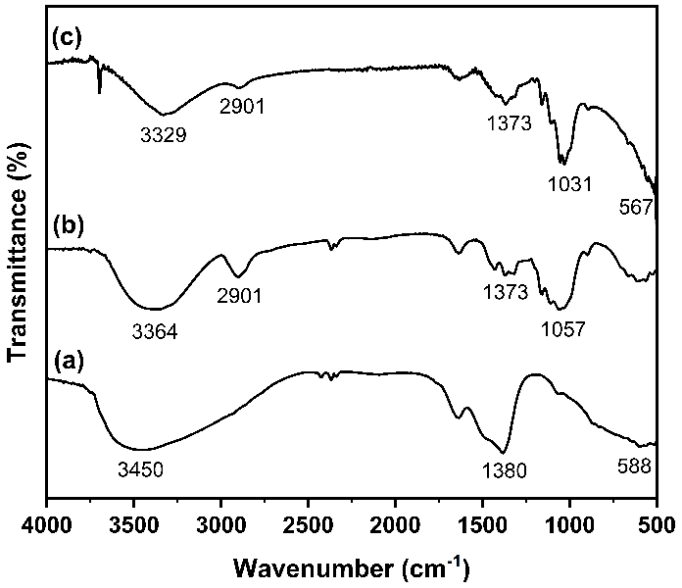

Figure 3. FT-IR Spectra of MgCr-LDH (a), MCC, and MgCr/MCC (c)

2. EXPERIMENTAL SECTION

2.1 Chemicals and Instrumentation

The materials used in this study such as $Mg(NO_3)_2.6H_2O$, $Cr(NO_3)_3.9H_2O$, sodium chloride (NaCl), and sodium hydroxide (NaOH) from EMSURE®, microcrystalline cellulose (MCC) from Merck, distilled water (H_2O) from Brataco,

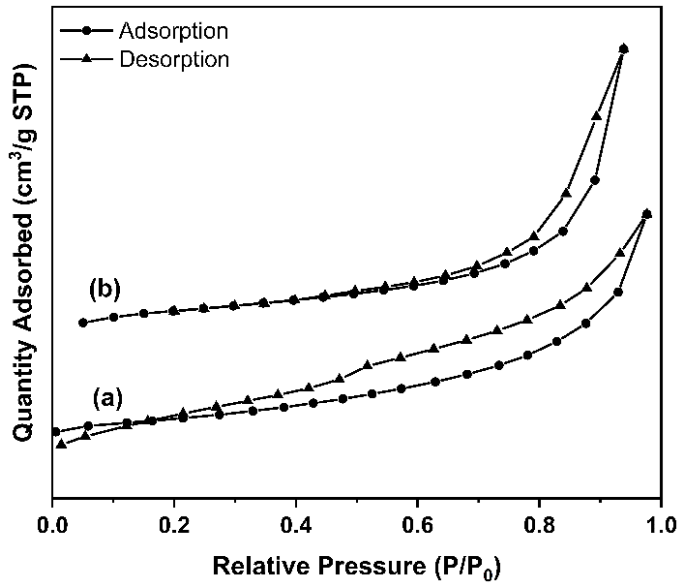

Figure 4. N_2 Adsorption-Desorption Properties of of MgCr-LDH (a) and MgCr/MCC (b)

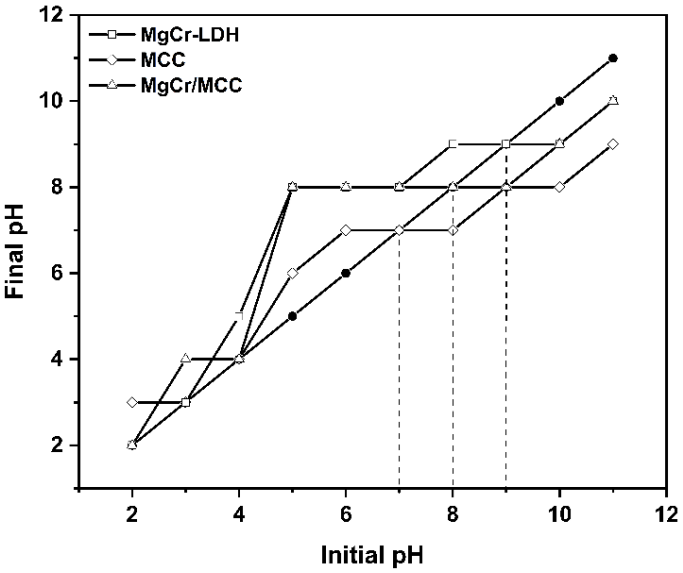

Figure 5. The Result of Determining pH pzc of the Materials

phenol (C_6H_5OH) from Sigma Aldrich, 4-amino antipyrine (C11H13N3O) from LOBA Chemie, potassium hexacyanoferrate (III) ($K_3[Fe(CN)_6]$) from PUDAK Scientific, buffer solution pH 10 from Smart-Lab, hydrochloric acid (HCl) from MallinckrodtAR®. The materials was characterized using an X-Ray Rigaku Miniflex-600 Diffractometer, Shimadzu Prestige-21 FTIR Spectrophotometer, BET Surface Area Analyzer Micrometric ASAP Quantachrome, and absorbance measurement of solution using Biobase Spectrophotometer UV-Visible BKUV1800PC.

Table 1. Results of BET Analysis Including Surface Area, Pore Diameter, and Pore Volume

Materials	Surface Area (m^2/g)	Pore Diameter (nm)	Pore Volume (cm^3/g)
MgCr-LDH	21.51	3.2	6.564
MgCr/MCC	26.056	6.272	0.082

2.2 Preparation of MgCr/MCC Composite

MgCr/MCC composite was prepared using the coprecipitation method with a constant pH (pH 10). $Mg(NO_3)_2.6H_2O$ 0.75 M and $Cr(NO_3)_3.9H_2O$ 0.25 M solutions totalling 30 mL each were added, and the pH was adjusted to 10 using a solution of NaOH 2 M. 1 g of MCC was then added after the mixture had been stirred for an hour. For three days, the solution is heated at an 80°C temperature. The precipitate was filtered, and the oven was used to dry it for 24 hours at 80°C. XRD, FT-IR, and BET studies were used to characterize the prepared materials.

2.3 pH point zero charge (pH pzc) and Adsorption Studies

Determination of pH pzc was carried out by adding 0.02 g of adsorbent into 20 mL of NaCl solution 0.1 M that has been adjusted to pH 2, 3, 4, 5, 6, 7, 8, 9, 10, and 11. The pH of a NaCl solution is adjusted by adding a 0.1 M solution of NaOH and HCl. After 24 hours of stirring, the liquid is filtered, and the filtrate's ultimate pH is measured with a pH meter. By plotting the correlation between the starting pH and final pH, the pHpzc of each substance was calculated.

The effects of pH, adsorption contact time, initial concentration, and temperature on the adsorption process were among the several treatments used in the adsorption investigation. By completing a phenol removal process on pH changes (2–11) with the purpose of determining the ideal pH in the adsorption process, the influence of pH adsorption may be explored. An Erlenmeyer containing 20 mL of phenol solution with a concentration of 10 mg/L was filled with up to 0.02 g adsorbents, and the mixture was stirred for two hours. By adjusting the contact time to find the optimum time, the effect of contact time adsorption on phenol may be studied. An Erlenmeyer containing 20 mL of phenol solution at a concentration of 10 mg/L, 0.02 g of adsorbents were added, and the mixture was stirred. By adjusting the concentration and temperature, the initial concentration and temperature adsorption impact was investigated. In an Erlenmeyer with 20 mL of phenol solution, up to 0.02 g of adsorbents were added, and the mixture was stirred for the optimum amount of time. With the use of a UV-Vis spectrophotometer, the filtrate was measured.

The phenol solution filtrate was complexed first before measuring its absorbance. A beaker glass containing up to 1 mL of phenol solution was then filled with up to 0.1 mL of a 2% solution of the 4-amino antipyrine reagent, 0.1 mL of an 8% solution of potassium hexacyanoferrate (III), 1 mL of a pH

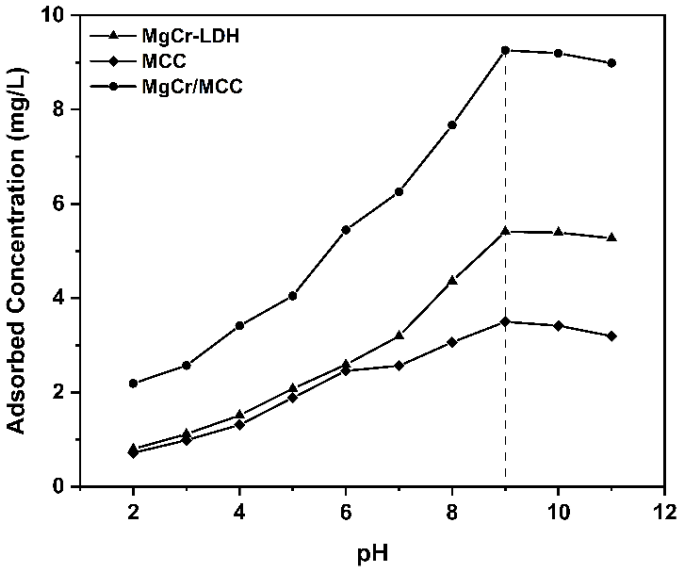

Figure 6. Effect of pH on the Phenol Removal

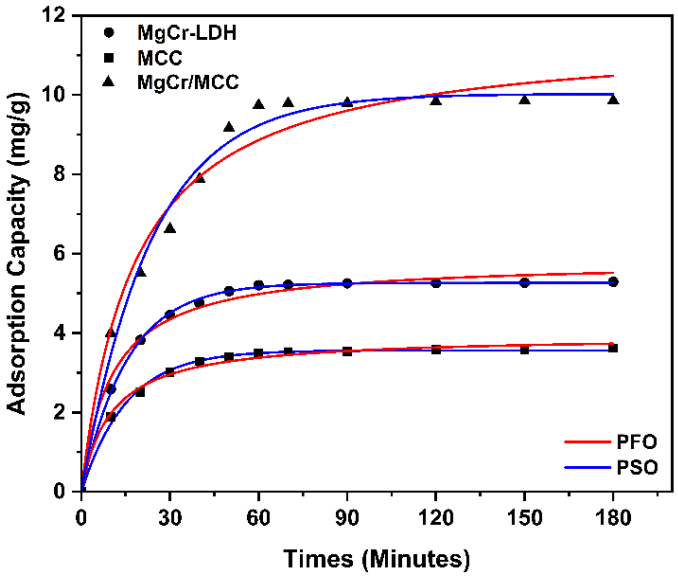

Figure 7. Effect of Contact Time and Adsorption Kinetic Models on the Phenol Removal

10 buffer solution, and 3 mL of distilled water. The mixture was then homogenized and left to stand for 15 minutes.

2.4 Regeneration Study

The adsorbent regeneration process occurs before the desorption process. Water is used in the desorption process, with the assist of an ultrasonic system (Figure 1). Following desorption, the regeneration procedure was carried out by adding 0.1 g of adsorbent to a phenol solution of 10 mg/L and stirring for 2 hours. The filtrate's absorbance was then evaluated using a UV-Visible spectrophotometer, and the adsorbent is then dried in an oven and then desorbed to be used in the next cycle regeneration process. In this study, a regeneration test of 5 cycles was carried out.

3. RESULT AND DISCUSSION

Figure 2 shows the results of the XRD characterization analysis. Based on Figure 2, MgCr-LDH has a diffraction peak at an angle of 11° (003), 22° (006), 36° (115), and 60° (110). The diffraction peaks in MCC shown in Figure 2 appear at diffraction angles of 15.2° (110), 22.7° (200), and 34.5° (004) which have similarities to the research conducted by Debnath et al. (2022). The success of the MgCr/MCC composite was determined by the appearance of LDH and MCC diffraction peaks in the composite material. The diffraction peaks appearing on the MgCr/MCC composite at diffraction angles of 15° (110) and 22.93° (200) are known to be typical peaks of MCC while the diffraction angle of 58.65° (110) is a typical peak of MgCr-LDH.

On the FT-IR spectra presented in Figure 3, the results of the FT-IR analysis can be seen. According to the FT-IR spectra shown in Figure 3, all materials had broadened vibrations between 3500 and 3200 cm^{-1}, which suggests the presence of a water molecule with a -OH group. The presence of metal bonds with oxygen is indicated by vibrations in MgCr-LDH materials that arise in the wave number range of 600–700 cm^{-1} and 1380–1380 cm^{-1}, respectively (M-O). The presence of aliphatic -CH from alkanes is indicated by vibrations in MCC regions between 3000 and 2850 cm^{-1}, while the existence of a C-O-C group in cellulose is indicated by vibrations in regions of 1030 cm^{-1}. Figure 3 shows what appears to be a typical vibration composed of MgCr-LDH and MCC materials: the MgCr/MCC composite material. The vibration that appears in the wave number range of 3000-2850 cm^{-1} (-CH aliphatic) and in the range of 1030 cm^{-1} (C-O-C) and in the region of about 1380 cm^{-1} (N-O) and in the region of about 600-700 cm^{-1} (M-O) is known as a characteristic vibration of LDH.

Figure 4 showed the N_2 adsorption-desorption properties of of MgCr-LDH and MgCr/MCC which exhibited type IV isotherm and a hysteresis phenomenon that classifies the material as having a mesoporous structure (Li et al., 2022). Table 1 shows that there is an increase in surface area in the MgCr-LDH material that has been modified with MCC to form MgCr/MCC, from 21.51 to 26.056 m^2/g. The pore sizes of the materials were 0.082 and 6.564 nm confirming that the mesoporous structure (<50 nm) and MgCr/MCC has a larger pore diameter. Based on these data, it can be confirmed that the modification of MgCr-LDH material with MCC improves the physical performance of the material.

Figure 5 shows the pH pzc of MgCr-LDH, MCC, and MgCr/MCC at pH 7, 8, 9, respectively. The pH pzc value can be known from the intersection of the lines at the initial pH and final pH. If the pH value of an adsorbent is below pH pzc, the adsorbent surface is positively charged, while if the pH value of an adsorbent is above pH pzc, the adsorbent surface

Table 2. Adsorption Kinetic Models Based on PSO and PFO for Phenol Removal

Materials	PFO			PSO		
	Qe (mg/g)	k_1 (min^{-1})	R^2	Qe (mg/g)	k_2 (g/mg min)	R^2
MgCr-LDH	2.492	0.039	0.889	5.562	0.025	0.998
MCC	1.680	0.032	0.900	3.800	0.040	0.999
MgCr/MCC	13.605	0.064	0.954	10.893	0.007	0.993

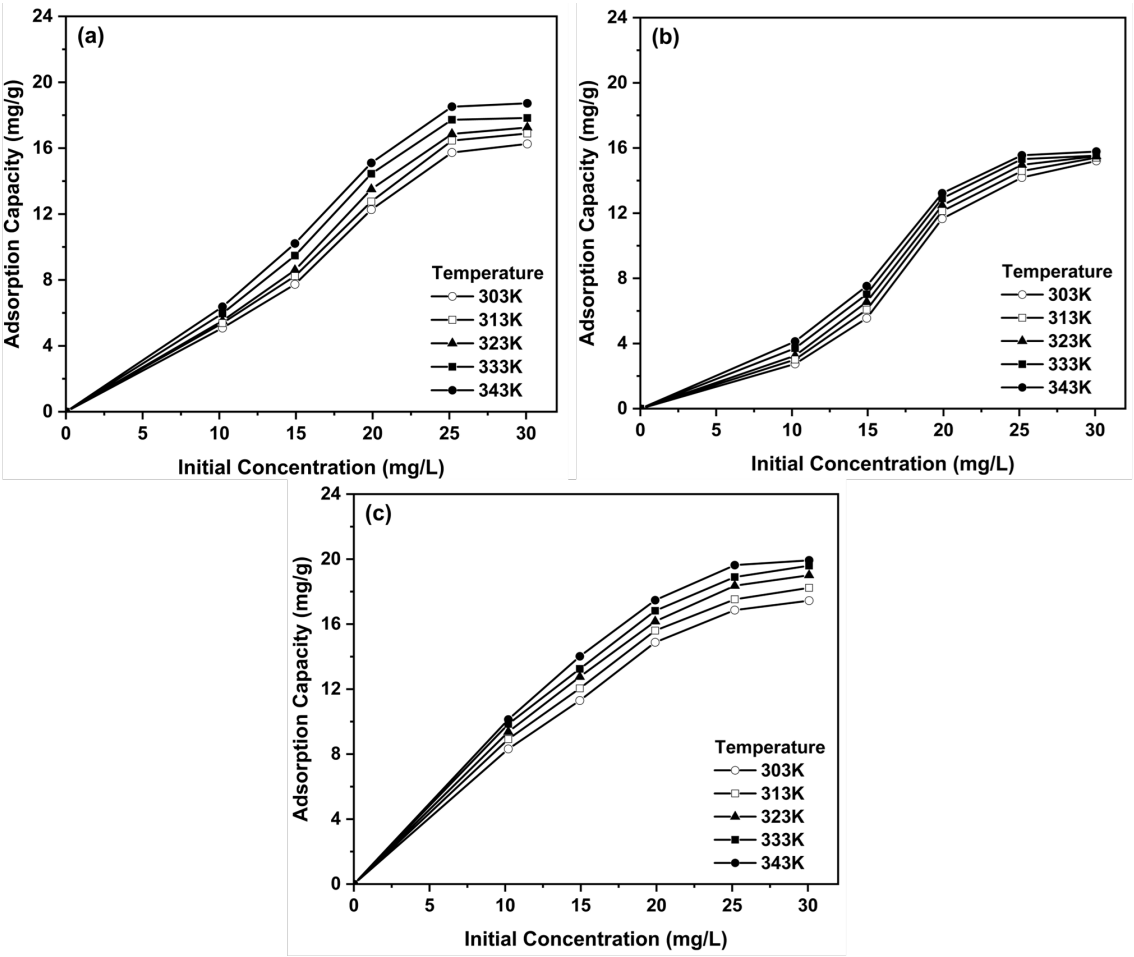

Figure 8. Effect of Initial Concentration and Temperature on the Adsorption Capacity of MgCr-LDH (a), MCC (b), and MgCr/MCC (c) for Phenol Removal

Table 3. Adsorption Isotherm Models for Phenol Removal

Materials	Adsorption Isotherm	Adsorption Constant	Temperature (°C) 30	40	50	60	70
MgCr-LDH	Langmuir	Qmax	24.631	24.450	22.523	21.097	21.882
		kL	0.149	0.180	0.273	0.484	0.569
		R^2	0.868	0.872	0.948	0.974	0.979
	Freundlich	n	0.688	0.738	0.791	0.932	1.024
		kF	3.612	2.510	1.812	1.014	1.460
		R^2	0.980	0.962	0.981	0.974	0.962
MCC	Langmuir	Qmax	6.930	9.540	13.240	7.100	8.100
		kL	0.050	0.050	0.040	0.100	0.112
		R^2	0.970	0.980	0.980	0.990	0.990
	Freundlich	n	0.410	0.460	0.500	0.590	0.700
		kF	13.900	11.200	10.500	7.240	4.400
		R^2	0.999	0.999	0.997	0.997	0.998
MgCr/MCC	Langmuir	Qmax	37.879	57.803	52.632	51.020	58.480
		kL	0.177	0.208	0.714	1.380	0.529
		R^2	0.988	0.996	0.998	0.998	0.999
	Freundlich	n	2.455	2.973	3.478	4.638	0.871
		kF	6.806	8.572	10.233	12.362	14.730
		R^2	0.924	0.943	0.960	0.973	0.983

Table 4. Thermodynamic Parameters for Phenol Removal

Materials	Concentration (mg/L)	T (K)	Qe (mg/g)	ΔH (kJ/mol)	ΔS (J/mol. K)	ΔG (kJ/mol)
MgCr-LDH	30.100	303	16.256	6.920	0.024	-0.381
		313	16.887			-0.622
		323	17.258			-0.863
		333	17.833			-1.104
		343	18.724			-1.344
MCC	30.100	303	15.210	1.500	0.005	-0.100
		313	15.403			-0.111
		323	15.500			-0.200
		333	15.523			-0.211
		343	15.800			-0.300
MgCr/MCC	30.100	303	17.443	7.800	0.029	-0.838
		313	18.232			-1.123
		323	19.011			-1.408
		333	19.596			-1.693
		343	19.929			-1.978

Table 5. Comparison of Adsorption and Regeneration Ability on the Phenol Removal by Several Adsorbents

Adsorbents	Adsorption Capacity (mg/g)	Regeneration Ability (Cycle)	Desorption Reagents	References
KOH-activated carbons from Brazil nut shell (1:0.5)	55.16	4	Ethanol	(Da Silva et al., 2022)
Magnetic Fe_3O_4/ZIF-8 composite	129.8	8	Methanol	(Qu et al., 2022)
Cationic surfactant modified attapulgite (Gemini modified ATP)	24.26	5	Ethanol	(Wang et al., 2020)
Zinc ferrite migration dependence on magnetic induce membrane	22	3	Sodium Hydroxide	(Said et al., 2021)
Porous carbon nanospheres aerogel based molecularly imprinted polymer	64.02	10	Ethanol/Acetic Acid	(Zhang et al., 2021)
Polyacrylonitrile nanofiber membranes	38.4	3	Ethanol and Sodium Hydroxide	(Nthunya et al., 2019)
Gelatin aerogel-containing Al-metal organic framework	16.56	4	Ethanol	(Kim et al., 2023)
MgCr/MCC	58.480	3	Water-assisted Ultrasonic System	This study

is negatively charged. In Figure 6, the optimum pH for all materials was at pH 9. According to Aisien et al. (2013), phenol is a weak acid (pKa = 9.89), where at pH values higher than the pka value will reduce the adsorption ability of the adsorbent caused by the repulsive force between the negatively charged adsorbent and phenolate ions in phenol. Buhani et al. (2018) revealed that at low pH, some phenols will be protonated and the adsorbent surface tends to be positively charged resulting in electrostatic repulsive forces so that the adsorption ability is weak. An increase in higher pH (pH>9) will cause excess -OH ions that will compete with phenolate ions on the adsorbent surface so that the adsorption ability is reduced. Based on data from the effect of pH on phenol removal, there are materials with an optimum pH obtained that is not the same as the pH pzc value of the material. This proves that the adsorption process does not only occur physically, there is chemical adsorption involvement between the adsorbent and adsorbate.

To illustrate the correlation between contact time and adsorption capacity, the pseudo first order (PFO) and pseudo second order (PSO) adsorption kinetics models were utilized in this research. According to Figure 7, the adsorption process reaches equilibrium after 70 minutes, with PSO following the adsorption kinetics by the value of the linear regression coefficient (R^2), which is close to the value of 1 (Table 2). The PSO model suggests that the chemical adsorption process might be the most dominant (Vinco et al., 2022).

Based on the graph in Figure 8, increasing concentration and temperature will cause phenol removal capacity to increase. Data on the effect of concentration and temperature variations on phenol removal were used to determine adsorption isotherm parameters and adsorption thermodynamics. Langmuir and Freundlich isotherm models are often employed isotherm models. The Langmuir adsorption isotherm model explains that the adsorption process occurs in a monolayer on the adsorbent surface with no interaction between adsorbate molecules (chemisorption) while the Freundlich adsorption isotherm model explains that the adsorption process occurs in a multilayer with the interaction between adsorbate molecules on the adsorbent surface so that with increasing concentration, the adsorption capacity also increases (physisorption) (Chen et al., 2022).

The correlation coefficient values in Table 3 show that the phenol removal process on MgCr-LDH and MCC materials follows the Freundlich isotherm (multilayer), while on MgCr/MCC follows the Langmuir isotherm (monolayer). The adsorption capacity values in Table 3 show that MgCr/MCC has a greater adsorption capacity than the initial material. The adsorption capacity of MgCr-LDH, MCC, MgCr/MCC materials are 24,631, 13,240, and 58,480 mg/g, respectively. Based on Table 4, the overall ΔG value is negative indicating a spontaneous adsorption process (Hu et al., 2021; Palapa et al., 2022) and ΔH value shows positively, which refers endothermic nature during the adsorption process (Brahma and Saikia, 2022).

Figure 9 shows the regeneration ability of materials on the

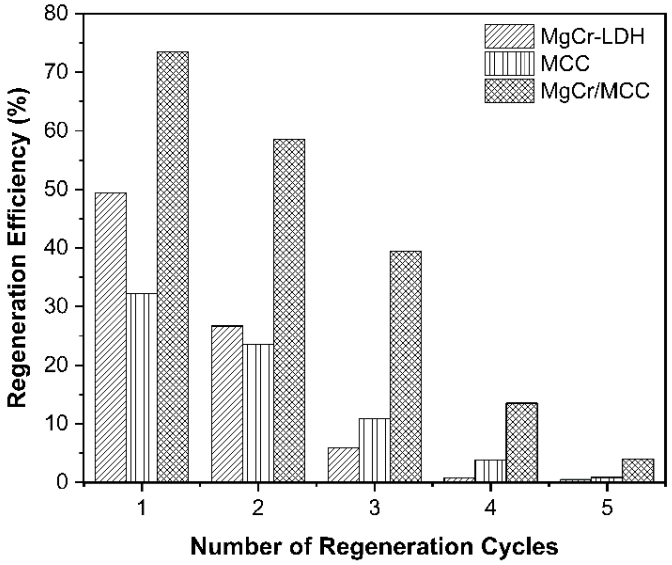

Figure 9. Regeneration Ability of Materials on the Phenol Removal

phenol removal, which in the fourth and fifth cycles shows a significant decrease in regeneration efficiency so that the material regeneration capability is 3 cycles. In the first cycle, the regeneration efficiency of MgCr-LDH, MCC, and MgCr/MCC materials was 49.4%, 32.2%, and 73.46%, respectively and in the third cycle, the regeneration efficiency decreased to 5.92%, 10.9%, and 39.45%, respectively. These data shows that the MgCr/MCC material has a higher regeneration ability than the initial material. The comparison of adsorption and regeneration ability on the phenol removal by several adsorbents showed in Table 5. The effectiveness of phenol removal can be seen by the value of adsorption capacity on MgCr/MCC which is quite large compared to other adsorbents. The regeneration ability of the MgCr/MCC material in phenol removal for 3 cycles which uses a desorption reagent, namely water, assisted by an ultrasonic system. The regeneration ability of the material in this study is not so high compared to the materials that have been reported using chemical reagents, but this study uses green desorption reagents which are more environmentally friendly because they only use water.

4. CONCLUSION

Preparation of MgCr/MCC was successful with characterized using XRD, FTIR, and BET analyses. MgCr/MCC showed an increase in surface area from 21.51 to 26.056 m^2/g and an increase in adsorption capacity from 24.631 to 58.480 mg/g. The regeneration ability of MgCr/MCC material using water-assisted ultrasonic system as a desorption reagent was 3 cycles with percent regeneration efficiency of 39.45%.

5. ACKNOWLEDGMENT

We would like to thank the Research Center of Inorganic Materials and Coordination Complexes, Faculty of Mathematics and Natural Sciences, Sriwijaya University for support and instrumental analysis.

REFERENCES

Abrishamkar, S., A. Mohammadi, J. De La Vega, D.-Y. Wang, and E. N. Kalali (2022). Layer-by-layer Assembly of Calixarene Modified GO and LDH Nanostructures on Flame Retardancy, Smoke Suppression, and Dye Adsorption Behavior of Flexible Polyurethane Foams. *Polymer Degradation and Stability*; 110242

Ahmad, N., F. S. Arsyad, I. Royani, and A. Lesbani (2023). Charcoal Activated as Template Mg/Al Layered Double Hydroxide for Selective Adsorption of Direct Yellow on Anionic Dyes. *Results in Chemistry*, **5**; 100766

Aisien, F., N. Amenaghawon, and R. Adeboyejo (2013). Potential Application of Recycled Rubber from Scrap Tire in the Removal of Phenol from Aqueous Solution. *Acta Technica Corviniensis-Bulletin of Engineering*, **6**(4); 127–133

Brahma, D. and H. Saikia (2022). Synthesis of ZrO_2/MgAl-LDH Composites and Evaluation of its Isotherm, Kinetics and Thermodynamic Properties in the Adsorption of Congo Red Dye. *Chemical Thermodynamics and Thermal Analysis*, **7**; 100067

Buhani, M. Puspitarini, Rahmawaty, Suharso, M. Rilyanti, and Sumadi. (2018). Adsorption of Phenol and Methylene Blue in Solution by Oil Palm Shell Activated Carbon Prepared by Chemical Activation. *Oriental Journal of Chemistry*, **34**(4); 2043–2050

Chen, X., M. F. Hossain, C. Duan, J. Lu, Y. F. Tsang, M. S. Islam, and Y. Zhou (2022). Isotherm Models for Adsorption of Heavy Metals from Qater-A Review. *Chemosphere*; 135545

Cho, B.-G., S.-B. Mun, C.-R. Lim, S. B. Kang, C.-W. Cho, and Y.-S. Yun (2022). Adsorption Modeling of Microcrystalline Cellulose for Pharmaceutical-based Micropollutants. *Journal of Hazardous Materials*, **426**; 128087

Da Silva, M. C., C. Schnorr, S. F. Lütke, S. Knani, V. X. Nascimento, É. C. Lima, P. S. Thue, J. Vieillard, L. F. Silva, and G. L. Dotto (2022). KOH Activated Carbons from Brazil Nut Shell: Preparation, Characterization, and Their Application in Phenol Adsorption. *Chemical Engineering Research and Design*, **187**; 387–396

Debnath, B., P. Duarah, D. Haldar, and M. K. Purkait (2022). Improving the Properties of Corn Starch Films for Application as Packaging Material via Reinforcement with Microcrystalline Cellulose Synthesized from Elephant Grass. *Food Packaging and Shelf Life*, **34**(8); 100937

Hasanah, M., Normah, A. Wijaya, F. S. Arsad, R. Mohadi, and A. Lesbani (2022a). High Selectivity and Adsorption Capacity for Congo Red Toward Anionic Dyes by Adsorbent: Modified LDH with Hydrochar Made from *Nephelium Lappaceum* Peel. *Global Nest Journal*, **24**(3); 487–494

Hasanah, M., A. Wijaya, F. S. Arsyad, R. Mohadi, and A. Lesbani (2022b). Preparation of C-based Magnetic Materials from Fruit Peel and Hydrochar using Snake Fruit (*Salacca zalacca*) Peel as Adsorbents for the Removal of Malachite Green Dye. *Environment and Natural Resources Journal*, **21**(1); 67–77

Haydari, I., A. Khalid, K. Sava, T. Daştan, N. Ouazzani, L. Mandi, and A. Faissal (2023). Green Synthesis of Reduced Graphene Oxide and Their Use On Column Adsorption of Phenol from Olive Mill Wastewater. *Process Safety and Environmental Protection*, **170**; 1079–1091

Hu, Y. Y., C. Pan, X. Zheng, F. Hu, L. Xu, G. Xu, Y. Jian, and X. Peng (2021). Prediction and Optimization of Adsorption Properties for Cs+ on NiSiO@ NiAlFe LDHs Hollow Spheres from Aqueous Solution: Kinetics, Isotherms, and BBD Model. *Journal of Hazardous Materials*, **401**; 123374

Iftekhar, S., V. Srivastava, and M. Sillanpää (2017). Synthesis and Application of LDH Intercalated Cellulose Nanocomposite for Separation of Rare Earth Elements (REEs). *Chemical Engineering Journal*, **309**; 130–139

Kim, T., K. Yun, N. Kim, B. Cha, J. Han, L. K. Njaramba, S. S. Elanchezhiyan, and C. M. Park (2023). Synthesis of Gelatin Aerogel-containing Al-metal Organic Framework for the Removal of Phenolic Contaminants from Aqueous Solutions. *Journal of Water Process Engineering*, **51**; 103441

Lammini, A., A. Dehbi, H. Omari, K. ELazhari, S. Mehanned, Y. Bengamra, Y. Dehmani, O. Rachid, A. A. Alrashdi, and O. Gotore (2022). Experimental and Theoretical Evaluation of Synthetized Cobalt Oxide for Phenol Adsorption: Adsorption Isotherms, Kinetics, and Thermodynamic Studies. *Arabian Journal of Chemistry*, **15**(12); 104364

Li, H., Q. Jin, J. Zhao, B. Wang, and X. Guo (2020). Rational Synthesis of a ZIF-67@ Co–Ni LDH Heterostructure and Derived Heterogeneous Carbon-based Framework as a Highly Efficient Multifunctional Sulfur Host. *Dalton Transactions*, **49**(36); 12686–12694

Li, Y., M. Wu, J. Wu, Y. Wang, Z. Zheng, and Z. Jiang (2022). Mechanistic Insight and Rapid Co-adsorption of Nitrogen Pollution from Micro-polluted Water Over MgAl-layered Double Hydroxide Composite Based on Zeolite. *Separation and Purification Technology*, **297**; 121484

Mahmoud, A. E. D., M. Franke, and P. Braeutigam (2022). Experimental and Modeling of Fixed-bed Column Study for Phenolic Compounds Removal by Graphite Oxide. *Journal of Water Process Engineering*, **49**; 103085

Mubarak, M. F., A. M. Zayed, and H. A. Ahmed (2022). Activated Carbon/Carborundum@ Microcrystalline Cellulose Core Shell Nano-composite: Synthesis, Characterization and Application for Heavy Metals Adsorption from Aqueous Solutions. *Industrial Crops and Products*, **182**; 114896

Nthunya, L. N., L. Gutierrez, S. Derese, B. B. Mamba, A. R. Verliefde, and S. D. Mhlanga (2019). Adsorption of Phenolic Compounds by Polyacrylonitrile Nanofibre Membranes: A Pretreatment for the Removal of Hydrophobic Bearing Compounds from Water. *Journal of Environmental Chemical Engineering*, **7**(4); 103254

Palapa, N. R., P. M. S. B. N. Siregar, A. Wijaya, T. Taher, and A. Lesbani (2022). High Selectivity and Stability Structure of Layered Double Hydroxide-Biochar for Removal Cd (II). *Bulletin of Chemical Reaction Engineering and Catalysis*, **17**(3); 520–532

Qu, Y., L. Qin, X. Liu, and Y. Yang (2022). Magnetic Fe_3O_4/ZIF-8 Composite as an Effective and Recyclable Adsorbent for Phenol Adsorption from Wastewater. *Separation and Purification Technology*, **294**; 121169

Rajamohan, N., S. Bosu, G. H. Ngo, and N. Al-Shibli (2022). Fabrication of Modified Carbon Nano Tbes Based Composite Using Ionic Liquid for Phenol Removal. *Molecular Catalysis*, **533**; 112792

Said, K. A. M., A. Ismail, A. Zulhairun, M. Abdullah, J. Usman, M. A. Azali, and M. A. Azali (2021). Zinc Ferrite Migration Dependence on Magnetic Induce Membrane for Phenol Removal: Adsorption Reaction and Diffusion Study. *Journal of Environmental Chemical Engineering*, **9**(1); 105036

Vinco, J. H., A. B. B. Junior, H. A. Duarte, D. C. R. Espinosa, and J. A. S. Tenório (2022). Kinetic Modeling of aAdsorption of Vanadium and Iron from Acid Solution through Ion Exchange Resins. *Transactions of Nonferrous Metals Society of China*, **32**(7); 2438–2450

Wang, K., X. Liu, J. Tang, L. Wang, and H. Sun (2020). Ball Milled Fe0@FeS Hybrids Coupled with Peroxydisulfate for Cr (VI) and Phenol Removal: Novel Surface Reduction and Activation Mechanisms. *Science of The Total Environment*, **739**; 139748

Wijaya, A., T. Taher, A. Lesbani, and R. Mohadi (2022). Variation of M2+ (Ni and Zn) in Cellulose-based M2+/Cr Composite Materials to Determine Adsorption and Regeneration Abilities on Phenol Removal. *Science and Technology Indonesia*, **7**(4); 461–468

Zhang, J., L. Qin, Y. Yang, and X. Liu (2021). Porous Carbon Nanospheres Aerogel Based Molecularly Imprinted Polymer for Efficient Phenol Adsorption and Removal from Wastewater. *Separation and Purification Technology*, **274**; 119029

Zhao, L., H. Zhang, B. Zhao, and H. Lyu (2022). Activation of Peroxydisulfate by Ball-milled α-FeOOH/biochar Composite for Phenol Removal: Component Contribution and Internal Mechanisms. *Environmental Pollution*, **293**; 118596

